ECE 445

SENIOR DESIGN LABORATORY

DESIGN DOCUMENT

Airloom Type Vertical Axis Wind Turbine

<u>Team #38</u>

CHENGSHENG JIANG
(jiang98@illinois.edu)
YIYANG ZHOU
(yiyang27@illinois.edu)
JIAYI GUO (jiayig8@illinois.edu)
JIAYAO LIN
(jiayaol3@illinois.edu)

TA: Yanbing Yang
Professor: Jiahuan Cui

April 13, 2025

Contents

1 Introduction

1.1 Problem

The world energy crisis has become an increasingly pressing issue as the demand for energy continues to rise worldwide while reserves of fossil fuel deplete[1], [2]. In response to this challenge, renewable energy have gained significant attention, among which wind energy stands out because of its abundance, sustainability, and pro-environment. Thus, harnessing wind energy through wind turbines offers a promising solution to lower the dependence on fossil fuels. However, vertical axis wind turbines (VAWTs) generally exhibit lower efficiency and Scaling up VAWTs for utility-scale applications remains difficult due to expensive structural construction cost and lower power output per unit.

Our design aims to enhance the efficiency of VAWT by changing the motion track of blades to be elliptical and designing energy conversion circuit of higher efficiency. Also, we try to use 3D-printing components to decrease the construction cost.

1.2 Solution

1.2.1 Mechanical Module

Mechanical Module is an elliptical lift-type VAWT to convert wind energy to mechanical energy. In details, using NACA0021 blades, wind generates positive work on blades under certain angles[3]. Blades are fixed on the HTD. Moving HTD drives pulley to rotate. Shaft of Aluminum is fixed with pulley and gives torque to generator.

1.2.2 Control Module

This control module has two main functions, boost voltage in order while maximizing efficiency, and manage batter while displaying data.

For voltage boosting and maximizing efficiency part, We plan to use a development board named CBB24210 (based on the STM microcontroller and boost circuit) to guarantee a fixed voltage output (provisionally set at 48V). This development board features a relatively complete hardware configuration and a heat dissipation function, which can reduce design risks.

For battery management and data display part, we are using EV2759-Q-01A, a highly integrated switching charger designed for portable devices with 1- to 6-cell series Li ion or Li polymer battery packs as battery management since it is also equipped with a protection mechanism. And we want to use a 5.5 inch LCD display real-time charging current (0A to 10 A with ±0.5A accuracy), voltage (40V to 60 V for 48V batteries with ±0.5V accuracy), and battery state of charge (SOC) (0% to 100% with ±1% accuracy).

1.3 Visual Aid

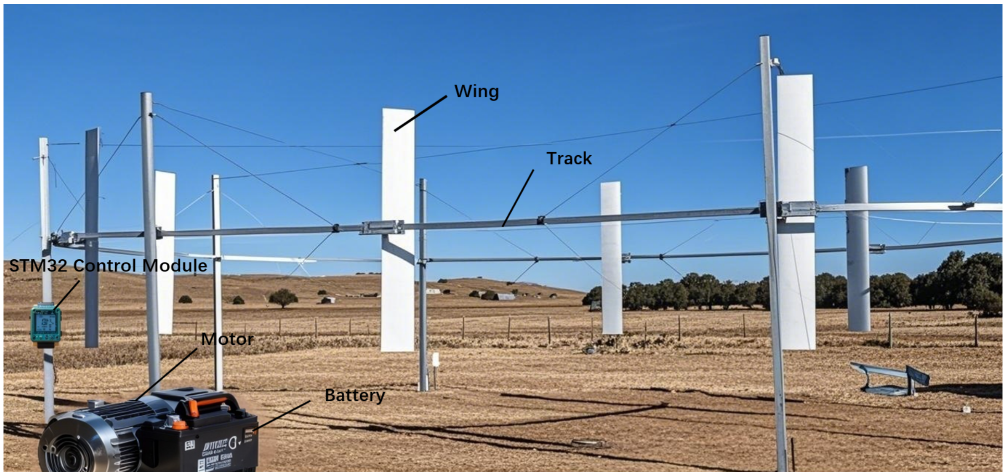

Figure 1: Visual aid

1.4 High-level requirements list

- With the wind speed of 9 m/s, tip speed ratio can reach 2 and VAWT can generate more than 200 W mechanical energy. Every component can bear the periodic force and be used for more than 1000h. The cost of construction should be less than 1500 yuan.
- The current rectification of the DC wind turbine generator will yield a fixed voltage output (provisionally set at 48V) which will be connected to the charging circuit. This circuit will use a boost circuit for voltage regulation and an MPPT algorithm to control the circuit output to enhance power generation efficiency.
- It must incorporate protection mechanisms to prevent overcharging, overdischarging,overcurrent, and overtemperature. In addition, the controller shall provide real-time monitoring of charging parameters, such as voltage, current, and temperature, via an LCD display, ensuring transparency and control over the charging process.

2 Design

2.1 Block Diagram

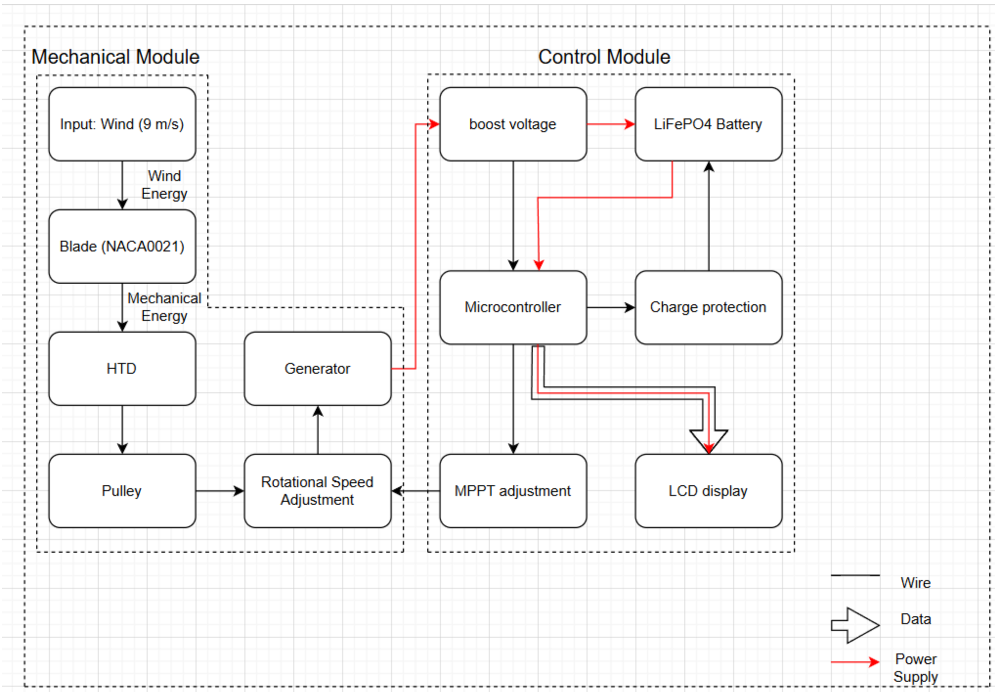

Figure 2: Airloom Type VAWT Flowchart

2.2 Physical Design

In the hardware design aspect, each module's implementation must be meticulously planned to ensure the entire system operates reliably and efficiently.

2.2.1 1. STM32 Microcontroller

An appropriate model of the STM32 microcontroller, such as the STM32F103 series, will be selected as the core processing unit of the system, providing ample peripheral interfaces and strong computational capacity. It will play a critical role in data acquisition, PWM modulation, and control commands.

2.2.2 2. ADC Module

The built-in ADC channels of the STM32 will be utilized to achieve real-time acquisition of output voltage and current from the generator. The resolution of the ADC (preferably 12 bits or higher) determines the precision of the measurements, enhancing the accuracy of the data captured.

2.2.3 3. Boost Converter Circuit

A DC-DC boost converter circuit will be designed, incorporating high-efficiency MOSFETs as switching elements and using energy storage principles. The voltage feedback loop will monitor the output voltage in real-time, providing the microcontroller with data to adjust the PWM signals accurately. The circuit layout will be optimized to reduce interference and ensure stable operation.

2.2.4 4. Charging Protection Circuit

This circuit will include battery voltage and current monitoring, typically employing operational amplifiers combined with current sensing methods to achieve precise monitoring. Integration of protection components such as fuses or electronic switches will safeguard the system by automatically disconnecting the circuit in the event of anomalies.

2.2.5 5. User Interface

A suitable LCD or OLED display module will be selected and connected to the STM32 via I2C or SPI interfaces. The program will be designed with a simple and understandable menu system, enabling users to easily comprehend the system state. Additionally, incorporating a buzzer or LED indicators will notify users of any malfunction, allowing for quick responses to issues.

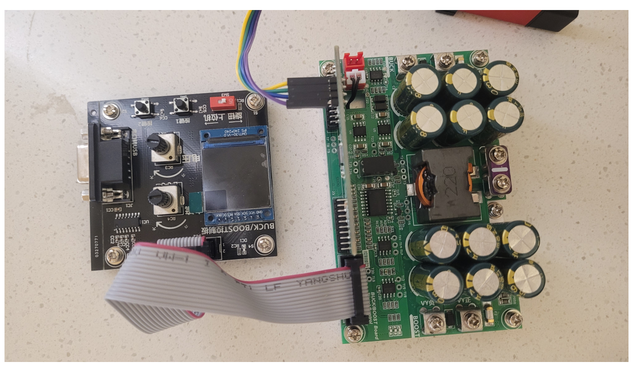

Figure 3: CBB02410, display module(left), control module(right)

2.3 Subsystem Overview

2.3.1 Subsystem 1: Blade, HTD, and pulley

Figure 4a illustrates the velocity field contours obtained from computational fluid dynamics (CFD) simulations at a tip speed ratio (TSR) of 2. For the conventional vertical axis wind turbine (VAWT), the wake structure displays a concentrated and relatively narrow region of low-velocity flow, represented by darker blue shades. The aerodynamic performance under this condition results in a mechanical power output of 97.59 W.

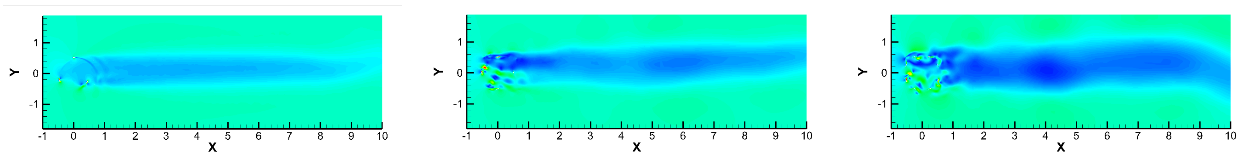

(a) Conventional VAWT (b) Four-bladed Square Rotor (c) Eight-bladed Square Rotor

Figure 4: CFD simulation results for different VAWT designs at TSR = 2

In the case of the four-bladed square-shaped rotor, as shown in Figure 4b, the CFD results indicate a noticeably darker and thicker low-velocity wake, signifying a more pronounced flow deceleration. By monitoring the force exerted on the wall surfaces of each blade and incorporating the blade rotational velocity derived from the TSR, the calculated mechanical power output is 88.28 W.

The eight-bladed square-shaped rotor, also simulated at TSR = 2, produces an even broader region of flow deceleration, with the dark blue wake extending across a larger area, as shown in Figure 4c. This suggests enhanced energy extraction from the airflow. Using the same force-based method to estimate mechanical energy conversion, the eight-bladed configuration achieves a significantly higher mechanical power output of 185 W. Based on these observations, the eight-bladed design was selected for further development due to its superior aerodynamic performance and energy conversion efficiency. In the ini-

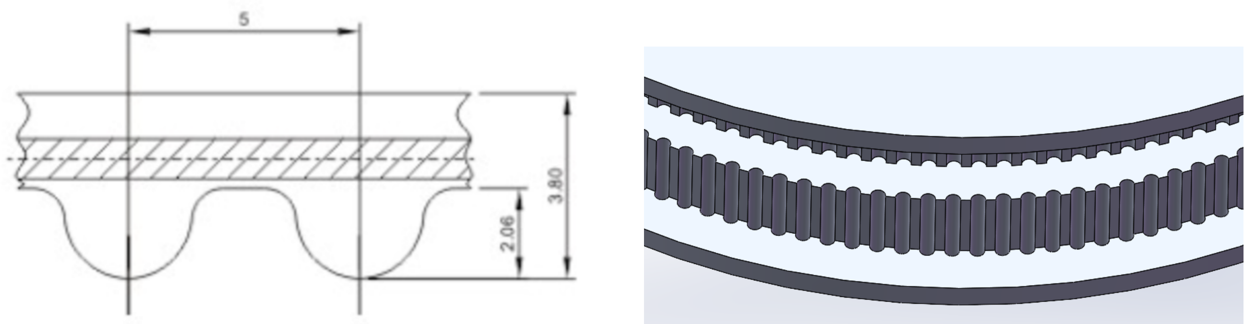

(a) HTD 5M Tooth profile by Jiebao (b) Pulley Model 1

Figure 5: First HTD 5M tooth profiles and Pulley

tial stage of this study, the HTD (High Torque Drive) tooth profile was obtained from a model provided by Ningbo Jiebao Power Transmission Systems Co., Ltd. As shown in Figure 5a[4], the manufacturer only supplied the geometric information of the tooth tip, while the geometry of the root region was missing. Consequently, we adopted a simplified modeling approach by omitting the root meshing region and focusing solely on the tooth tip portion. Based on the available data, a preliminary pulley model was constructed to match the provided tooth tip geometry, as illustrated in Figure 5b. A total of 162 holes were excavated, with each hole located at an equal distance from the next. The radius of the circle was measured to be 128.75 mm, and the point on the side was designated as the centre of the circle, with a radius of 2.98 mm, for the purpose of synchroniser wheels.

Initial static fitting tests showed that the teeth of the pulley aligned well with the timing belt, resulting in a seemingly accurate one-to-one engagement between the mating surfaces. However, when the pulley was tested under rotational conditions within the wind turbine generator, we observed frequent occurrences of tooth skipping. This led to undesirable friction and slippage, significantly impairing the efficiency of mechanical energy conversion from wind energy.

Upon further review, we discovered that most manufacturers do not publish detailed HTD profile geometries. Publicly available sources, such as norelem[5], only provide general tooth parameters without disclosing exact construction details. To reconstruct the HTD 5M profile more accurately, we referred to published profile diagrams and practical engineering experience. We interpreted the tooth shape as comprising three distinct segments: a circular arc at the tooth tip, a transitional straight flank, and a root fillet arc. This geometry is illustrated in Figure 6a. To validate the feasibility of this reconstructed profile, we fabricated a prototype pulley using 3D printing techniques. A static fit test with the timing belt showed a significantly improved engagement, as depicted in Figure 6b. Encouraged by this result, the next phase of this research will focus on evaluating the dynamic performance of the belt-pulley system under continuous operation, specifically monitoring for any remaining instances of tooth skipping or abnormal friction.

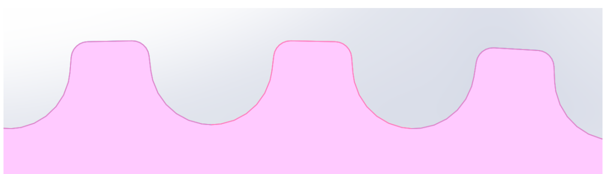

(a) Estimated HTD 5M Tooth profile

(b) Fit Test

Figure 6: Estimated HTD 5M tooth profiles and Fit Test

2.3.2 Subsystem 2: Base and Motor

System Architecture The design architecture of this circuit control system consists of five core components: the DC generator, boost circuit, Maximum Power Point Tracking (MPPT) module, charging control module, and user display interface. These components work together to achieve efficient utilization and management of wind energy.

1. Base The base of the vertical axis wind turbine (VAWT) is constructed using aluminum profiles, chosen for their excellent modularity, structural integrity, and ease of assembly. The frame serves as the primary load-bearing structure that supports the four vertical shafts and the associated bearings, which in turn stabilize and guide the motion of the blade rotation system. Each corner is reinforced with vertical members to enhance rigidity and resist torsional deformation caused by the rotating blades and generator torque.

Bearings are inserted into 3D-printed sockets and seated within circular holders integrated into the top and bottom aluminum profiles. These guide and stabilize the vertical shafts, minimizing vibration and allowing for smooth elliptical blade motion. The use of modular extrusions also facilitates quick adjustments during testing, such as repositioning the motor or tuning shaft alignment.

To accommodate the DC motor and generator assembly, a dedicated compartment is built into the lower front section of the base. The DC motor and generator are mounted to the base using sliders and corner brackets that match the slot profiles. This method allows for precise and flexible adjustment of the motor position and belt tension without the need for custom machining. The modular design further simplifies maintenance and replacement, as components can be detached or repositioned with minimal effort. Cable routing pathways are planned through the inner channels of the T-slot profiles to ensure a clean and safe electrical layout.

2. DC Generator Serving as the energy source for the system, the selected 24V DC generator generates electrical energy driven by wind. The output voltage of the generator directly correlates with wind speed; as wind speed increases, the output voltage rises accordingly. Thus, the design must take into account the output characteristics of the generator to adapt to varying environmental conditions effectively.

3. Boost Circuit To meet the charging requirements of the battery, a boost conversion circuit is designed. This component will elevate the 24V output voltage through PWM modulation and energy storage in inductors to a suitable charging voltage (e.g., 36V or higher) for various battery types (like lithium-ion or lead-acid). High-efficiency MOSFETs and appropriately sized inductors are selected to minimize power loss and thermal degradation.

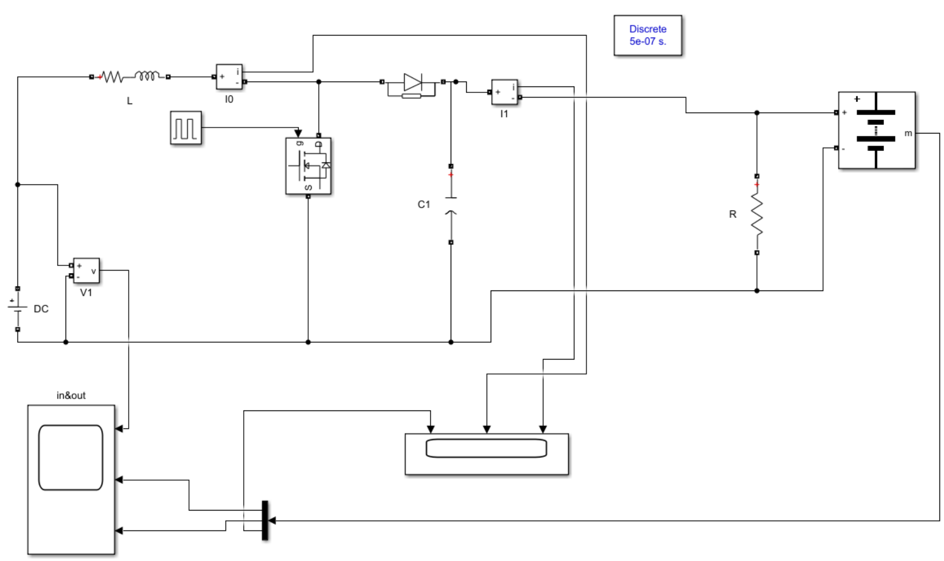

Figure 7: Boost simulation

3. MPPT Algorithm Module The MPPT technology continuously adjusts the system's working point to extract the maximum output power from the wind turbine. Algorithms such as Perturb and Observe will be implemented in the STM32 microcontroller, which periodically adjusts the PWM signal and monitors the voltage and current output from the generator to compute power. The microcontroller responds quickly to changes in power to maintain operation at the optimal point, thereby improving the overall efficiency of the system.

4. Charging Control Module This module intelligently adjusts the current delivered to the battery based on its charging state. It encompasses voltage monitoring, overcharge protection, over-discharge protection, and short-circuit protection functionalities. When the battery is fully charged, the system automatically stops charging to prevent overcharging. Conversely, it restricts output when the battery charge drops below a preset threshold to safeguard battery longevity.

5. User Display Interface To facilitate user monitoring of the system's status, an intuitive display interface is designed using an LCD or OLED screen. This screen will show real-time information, such as battery voltage, current output, power status, and operational time.

2.4 Tolerance Analysis

For the Frame and Aluminum Extrusion Assembly, aluminum profiles were cut with a dimensional tolerance of ±0.5 mm. To ensure consistent frame geometry, all components were measured and adjusted before final fastening. Angle brackets and three-way connectors inherently allow for slight tolerance absorption, and any accumulated error is corrected during the squaring and alignment process.

The timing pulley and belt require accurate pitch alignment and concentricity to prevent tooth skipping during operation. Pulley teeth were modeled with tolerances within ±0.1 mm on the tooth profile. Additionally, for DC generator, belt tension is adjusted via a motor mounting slot mechanism, with a travel range of ±5 mm. This allows compensation for small length tolerances in the belt and maintains optimal engagement force.

In the design of our mechanical structure, the primary tolerance consideration lies in the fit between 3D-printed components and selected standard parts. Based on empirical observations, the 3D printing process typically results in an edge deviation of approximately 0.12 mm. To ensure proper assembly fit, we have implemented the following compensatory measures in our design:

For internal diameters (IDs), we systematically increase the nominal dimension by 0.12 mm For external diameters (ODs), we correspondingly decrease the nominal dimension by 0.12 mm This compensation strategy effectively accommodates the characteristic dimensional variation inherent in the additive manufacturing process while maintaining functional compatibility with standard components.

One crucial aspect of the design is the boosting and charging functionality. Our STM32 microcontroller is engineered to reject any power output from the motor that is below 12V and boost it to a maximum of 48V, with a current limit of 5A, for battery charging. The specific characteristics of the boost output can vary according to the battery's condition to enable staged charging.

However, ensuring high battery - charging efficiency is of utmost importance as it directly impacts the utilization efficiency of wind energy. To this end, we conducted tests using an electronic load and a DC power supply (24V 10A). Under conditions of constant voltage, constant current and with rated resistances (1 ohm, 4 ohm, 8 ohm, 12 ohm), we determined that the efficiency loss between the output and input does not exceed 25%.

3 Cost and Schedule

3.1 Cost

Table 1: Material Cost Table from Dec.21th to Apr.13th

Time	Item	Description	Quantity	Price
12/21	HTD 5M	1000, 30	1	30
1/7	Carbon fibre tube	OD 4mm, ID 2mm, L 1m	4	27.24
1/7	Step screw	semi-toothed 6 * 16 * M5	5	9.41
1/9	Kafuter	70g	1	8
2/26	PLA	K5-1.75-WHT-1KG	5	400
3/3	DC Generator	DC 300W	1	200.04
3/6	Screw	M4 * 55	10	2.8
3/6	Nut	M4	100	2.62
3/6	Bearing	32*52*20	2	50
3/11	HTD 5M	3900, 30	2	220
3/11	Al tube	1500*32	4	160
3/12	Bearing	32*52*20	3	67.5
3/17	Bearing	40*62*12	8	34.4
3/18	Carbon fibre tube	OD 4mm, ID 2mm, L 1m	4	27.24
3/26	3-way aluminum corner bracket	30*30*30	16	93.12
3/26	Bearing	Sliding Bearings	4	18.18
3/27	Bearing	51407/P5 35*80 *32	4	95.04
4/8	Aluminum profile	10m	1	330.9

Table 2: Labor Cost Table from Dec.21th to Apr.13th

Task	Hours	Rate (¥/hour)	Price
SolidWorks Designing	30	100	3000
3D Print	6	70	420

Assemble	10	100	1000
PCB Designing	20	100	2000
PCB Debugging	15	100	1500
Documentation	18	50	900

3.2 Schedule

Table 3: Schedule Table from Dec.21th to Apr.20th

Week of	**Plan**	**Member**
Dec 21, 2024	CFD	C.S.J
Jan 21, 2024	Design blade	C.S.J
Jan 21, 2025	Design base	Y.Y.Z
Feb 20, 2025	1th PCB Designing	J.Y.G J.Y.L
Feb 20, 2025	DC motor choose	Y.Y.Z
Feb 20, 2025	Design pulley	C.S.J
Mar 1, 2025	2th PCB Designing	J.Y.G J.Y.L
Mar 18, 2025	Design connection	Y.Y.Z C.S.J
Mar 20, 2025	PCB debudgging	J.Y.G J.Y.L
Apr 10, 2025	Assemble	Y.Y.Z C.S.J
Apr 10, 2025	3th PCB Designing	J.Y.G J.Y.L

4 Ethics and Safety

4.1 Ethics

4.1.1 Following the IEEE Code of Ethics

As a project team, we're committed to following the IEEE Code of Ethics[6]. This means being honest and respectful in all our communications about the project, including our goals, methods, and outcomes.

4.1.2 Caring for the Environment

Our wind energy system will be designed with sustainability, striving to minimize its environmental impact. By focusing on renewable energy, we're playing our part in conserving the environment, which aligns with IEEE's vision of using technology for the greater good.

4.1.3 Integrity in Research

The research and data collection we conduct will be guided by ethical standards. We'll make sure to cite all our sources properly and present our data honestly, avoiding any kind of misrepresentation.

4.1.4 Respecting Intellectual Property

We'll respect intellectual property rights by obtaining necessary permits and licenses for the technologies we use. It's also essential to acknowledge the contributions of others in our research and project development.

4.2 Safety

4.2.1 Following IEEE Safety Standards

During the design and implementation of our project, we'll adhere to relevant IEEE safety standards, like IEEE 1547, which deals with connecting distributed resources to electric power systems. This compliance is crucial for preventing electrical safety hazards.

4.2.2 Conducting a Risk Assessment

We'll perform a detailed risk assessment to pinpoint potential hazards that could arise during the installation and operation of the wind energy system, such as electrical issues, mechanical failures, and environmental impacts.

4.2.3 Electrical Safety Protocols

We'll only use electrical components that meet established safety standards. Safety features, like circuit breakers, fuses, and grounding systems, will be included to reduce electrical hazards.

4.2.4 Preparing for Emergencies

Developing and communicating emergency response plans for potential issues, like mechanical failures or severe weather, is essential. Everyone involved will be trained on these plans to ensure effective action if something goes wrong.

references

[1] P. Papon, "Aie (agence internationale de l'énergie). World Energy Outlook 2024, paris : Aie, octobre 2024, 398 p.," *Futuribles*, no. 464, pp. 140–143, 2025, https://iea.blob.core.windows.net/assets/6a25abba-1973-4580-b6e3-ba014a81b458/WorldEnergyOutlook2024.pdf, Consulté le 28 novembre 2024. [Online]. Available: https://shs.cairn.info/revue-futuribles-2025-1-page-140?lang=fr.

[2] M. M. Rienecker, M. J. Suarez, R. Gelaro, *et al.*, "MERRA: NASA's Modern-Era Retrospective Analysis for Research and Applications," *Journal of Climate*, vol. 24, no. 14, pp. 3624–3648, 2011, Web. DOI: 10.1175/JCLI-D-11-00015.1. [Online]. Available: https://doi.org/10.1175/JCLI-D-11-00015.1.

[3] R. E. Sheldahl and P. C. Klimas, "Aerodynamic characteristics of seven symmetrical airfoil sections through 180-degree angle of attack for use in aerodynamic analysis of vertical axis wind turbines," Sandia National Laboratories, Technical Report, 1981, SAND80-2114, pp. 52–62.

[4] Ningbo Jiebao Power Transmission Systems Co., Ltd., *Htd 5m tooth profile diagram*, Included in physical product manual, Accessed in April 2025, 2024.

[5] norelem USA. "Toothed belt profile htd 5m." (2025), [Online]. Available: https://www.norelemusa.com/en-us/Product-Overview/Systems-and-components-for-machine-and-plant-construction/22000/Toothed-belts-toothed-belt-pulleys/Toothed-belt-profile-HTD-5M/p/agid.18242 (visited on 04/13/2025).

[6] I. S. Association. """IEEE Standard 7000-2021: Model Process for Addressing Ethical Concerns during System Design"." (2021).

[7] L. You. "Zero-carbon technology: New designs reduce the cost of wind power." Online; accessed 14-April-2025. (2023), [Online]. Available: https://zhuanlan.zhihu.com/p/670498010.